

# Facile Preparation of Cationic P (St-BA-METAC) Copolymer Nanoparticles and the Investigation of Their Interaction with Bovine Serum Albumin

Penghui Li,<sup>1</sup> Xiaoxi Hu,<sup>1</sup> Gongwu Song,<sup>1</sup> Paul K. Chu,<sup>2</sup> Zushun Xu<sup>1</sup>

<sup>1</sup>Ministry-of-Education Key Laboratory for the Green Preparation and Application of Functional Materials, College of Materials Science and Engineering, Hubei University, Wuhan 430062, China

<sup>2</sup>Department of Physics and Materials Science, City University of Hong Kong, Tat Chee Avenue, Kowloon, Hong Kong, China

Received 8 June 2010; accepted 20 September 2011

DOI 10.1002/app.35676

Published online 28 December 2011 in Wiley Online Library (wileyonlinelibrary.com).

**ABSTRACT:** Cationic copolymer nanoparticles were prepared by emulsifier-free emulsion polymerization of styrene and *n*-butyl acrylate, using [2-(methacryloyloxy ethyl) trimethylammonium chloride as the cationic functional comonomer and 2,2'-azobis (2-methylpropanimidine) as the cationic initiator. FTIR spectroscopy, <sup>1</sup>H-NMR spectroscopy, and GPC were applied to characterize the chemical structure and molecular weight of the obtained copolymer. The size and size distribution of the nanoparticles were characterized through photon correlation spectroscopy. The interaction of nanoparticles with bovine

serum albumin (BSA) was investigated by the means of transmission electron microscopy and fluorescence spectroscopy. It was found that the copolymer nanoparticles were monodisperse spheres with the diameter less than 90 nm and can complex well with BSA through electrostatic interaction. © 2011 Wiley Periodicals, Inc. *J Appl Polym Sci* 125: 864–869, 2012

**Key words:** cationic copolymer; nanoparticles; BSA; fluorescence spectroscopy

## INTRODUCTION

Polymer nanoparticles with specific shape and unique surface functionalities, especially those with charged groups ( $-\text{SO}_3^{2-}$ ,  $-\text{COO}^-$ , and  $-\text{N}^+(\text{CH}_3)_3$ ) and reactive groups ( $-\text{COOH}$ ,  $-\text{OH}$ ,  $-\text{NH}_2$ , and  $-\text{SH}$ )<sup>1</sup> are offering useful supports in varied fields for many years. As a result, researches dedicated to the design, preparation, and application of the functional polymer nanoparticles are increasingly prosperous currently.<sup>2–4</sup>

In recent years, marvelous studies focused on cationic charged polymer nanoparticles are being carried out. Monomers with amino groups and the derivatives, especially ones bearing quaternary ammonium groups, are the most applied compositions in the design and synthesis of cationic polymer nanoparticles. And approaches for the preparation of them were universally reported recently, such as methods based on emulsion polymerization,<sup>5,6</sup> polyelectrolyte complexation technique,<sup>7</sup> and self-assem-

ble of amphiphilic copolymers.<sup>8</sup> Among them, emulsifier-free emulsion polymerization is a simple and mature technique to prepare polymer nanoparticles and owns obvious advantages. The absence of surfactant in the system offers the possibility to obtain rather “clean” polymer nanoparticles,<sup>9</sup> avoiding the interference of surfactant during property measurements and even in the applications afterwards. Meanwhile, in the process of emulsifier-free emulsion polymerization, the use of ionic initiator ensures the colloid stabilization and surface charge density of polymer nanoparticles.<sup>10</sup>

Because of the ability to interact with fibers,<sup>11,12</sup> cements,<sup>13</sup> and pollutants in waste water,<sup>14</sup> cationic polymer nanoparticles are widely applied in fields like paper industry, textile or fabric finishing, and sewerage treatment. Furthermore, positive charged nanoparticles can complex with phosphate groups in DNA molecules and negative charged proteins through electrostatic interaction. Thus, cationic polymer nanoparticles also possess the potentiality of applications in biotechnology fields, including protein separation,<sup>15</sup> protein carriers,<sup>16</sup> and medical diagnostics.<sup>17</sup>

As have been well known, proteins are of significant importance in organism and are the main component of large numbers of medical drugs nowadays. To apply various materials in the biomedical

Correspondence to: Z. Xu (zushunxu@hubu.edu.cn).

Contract grant sponsor: Specialized Research Fund for the Doctoral Program of Higher Education of China; contract grant number: 20094208110002.

field, studies on the interaction between proteins and other materials seem to be increasingly urgent.<sup>18–20</sup> Because of the presence of functional groups like  $-\text{COOH}$  and  $-\text{NH}_2$  in the same molecule, proteins exhibit the property of amphoteric ionization and isoelectric point (pI), the pH value at which the molecule carries no electrical charge. At a pH below their pI, proteins carry net positive charge, whereas above their pI they carry net negative charge.<sup>21</sup> That is to say, the net electrical charge of proteins highly depends on the pH values of their surrounding environment. Thus, by appropriately adjusting the pH value, negative charged proteins can be obtained and can certainly be made to bind to the surface of cationic nanoparticles.

In this study, functional cationic comonomer [2-(methacryloyloxy) ethyl] trimethyl ammonium chloride (METAC) was used to introduce positive charge into polymer nanoparticles. Nanosized, surface clean, narrow distributed cationic copolymer nanoparticles were prepared by emulsifier-free emulsion polymerization. And their interaction with protein, bovine serum albumin (BSA) as the model in this set of experiment, was preliminarily investigated by transmission electron microscopy (TEM) and fluorescence spectra. The objective is to explore the prospect of the application of polymer nanoparticles as the protein carriers and drug delivery.

## EXPERIMENTAL

### Materials

All the chemical reagents were analytical grade. Styrene (St) and *n*-butyl acrylate (BA) were distilled under reduced pressure to remove the inhibitors and stored at 4°C before use. An aqueous solution (75 wt %) of [2-(methacryloyloxy) ethyl] trimethyl ammonium chloride (METAC) was purchased from Aldrich and used as received. 2,2'-Azobis(2-methylpropionamide) dihydrochloride (AIBA) was supplied by Acros Organics Co. and purified by recrystallization. Acetone and  $\text{CaCl}_2$  were analytical grade and used without further purification.

Bovine serum albumin (BSA, average molecular weight of 66,000 g/mol) was supplied by Beijing Shuangxuan Biological Culture Medium Plant (Beijing, China). The stock solution of BSA was prepared by dissolving BSA in distilled water and stored at 0–4°C. The concentration of working solution of BSA was  $1 \times 10^{-5}$  mol/L.

### Preparation of cationic copolymer nanoparticles

The preparation of cationic polymer nanoparticles was carried out by typical emulsifier-free emulsion polymerization. The procedure can be described as

follows: St (2.34 g, 22.47 mmol), BA (2.00 g, 15.60 mmol), comonomer METAC (0.2955 g, 1.423 mmol), and distilled water were poured into a 250-mL four-neck round-bottom flask equipped with a reflux condenser, a Teflon paddle stirrer, and bubbled with a fine stream of nitrogen. After sufficiently dispersing at 45°C for 30 min, AIBA (0.04 g, 0.1475 mmol) was added in to initiate the reaction. Continuous copolymerization proceeded for 8 h at 73°C. Then, the mixture was cooled to room temperature to get the resulting emulsion.

Certain amount of the resulting emulsion was dialyzed for 72 h in the dialysis bag against 1000 mL deionized water, which was exchanged at an interval of 12 h. The dialyzed emulsion was deposited in the mixture of acetone and  $\text{CaCl}_2$  solution. Then, the product was collected by filtration, washed three times with acetone and distilled water, and then dried under vacuum at 40°C. P (St-BA-METAC) copolymer was obtained.

### Measurements

#### FTIR spectroscopy

FTIR spectrum of the copolymer was performed on the Perkin-Elmer Spectrum one Transform Infrared Spectrometer (Perkin-Elmer, USA). The copolymer film was cast onto KBr disk, and the FTIR spectrum was recorded from 4000 to 450  $\text{cm}^{-1}$ .

#### Nuclear magnetic resonance spectroscopy

The nuclear magnetic resonance ( $^1\text{H-NMR}$ ) spectrum of the copolymer was recorded using a UNITY INVOA-600 MHz spectrometer (Varian, USA) at 20°C with  $\text{CDCl}_3$  as the solvent. Chemical shifts were reported in ppm units with tetramethylsilane as an internal standard.

#### Molecular weight and molecular weight distribution

The molecular weight and molecular weight distribution of the copolymer were measured on a Waters 150-C gel permeation chromatograph (GPC) equipped with polystyrene gel columns (HT2, HT3, and HT4) at 30°C. THF was used as eluant, and polystyrene standards were used as calibrations.

#### Transmission electron microscopy

The morphology of the nanoparticles and that of nanoparticles interacted with BSA were characterized by TEM (Tecnai G20, FEI Corp. USA). A drop of diluted sample was placed on a carbon-coated copper grid and dried in air. The TEM images were obtained at 25°C at an electron acceleration voltage of 200 kV.

### Size and zeta potential determination

The average hydrodynamic radius ( $R_h$ ) and size distribution (Polydispersity index) of obtained nanoparticles with the absence and presence of BSA were measured by photon correlation spectroscopy (PCS) (Auto size Loc-Fc-963, Malvern Instrument). The dialyzed dispersion of copolymer nanoparticles interacted with BSA were diluted with deionized water to get an appropriate concentration and then poured into a cuvette. The cuvette was set inside a sample holder. The temperature of the holder was maintained at a desired temperature of 25°C, and the diluted dispersions were measured at 90° scattering angle. The value of "Polydispersity Index" ranged between 0 and 1, and a smaller value of "Polydispersity Index" meant narrower particle size distribution.

The zeta potential measurements were carried out using a Malvern NanoZS, model ZEN 3600 (Malvern Instruments, UK). Each sample was properly diluted with ultrapure water, and pH value was adjusted to 7.4 with PBS buffer.

### Fluorescence spectroscopy

The fluorescence properties of a series of copolymer nanoparticles interacted with BSA molecules were studied on a RF-540 spectrometer (Hitachi high-technologies corp., Tokyo, Japan). A total of 50  $\mu$ L dialyzed dispersion of copolymer nanoparticles and BSA solutions of different concentration were added into a 25-mL volumetric flask, and the pH value was adjusted to 7.01 with tris buffer. The mixture was diluted to 25 mL with doubly distilled water and vortexes. The fluorescence emission spectra were recorded in the wavelength range 350–500 nm at the exciting wavelength of 280 nm. Both the excitation and emission slits were 5 nm.

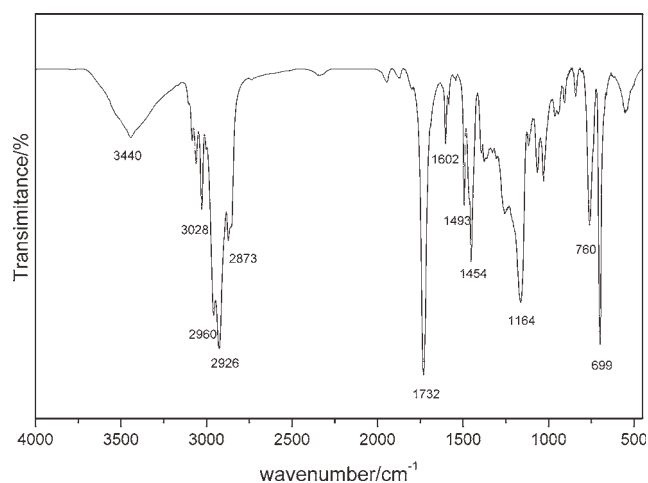


**Figure 1** FTIR spectrum of P (St-BA-METAC) copolymer.

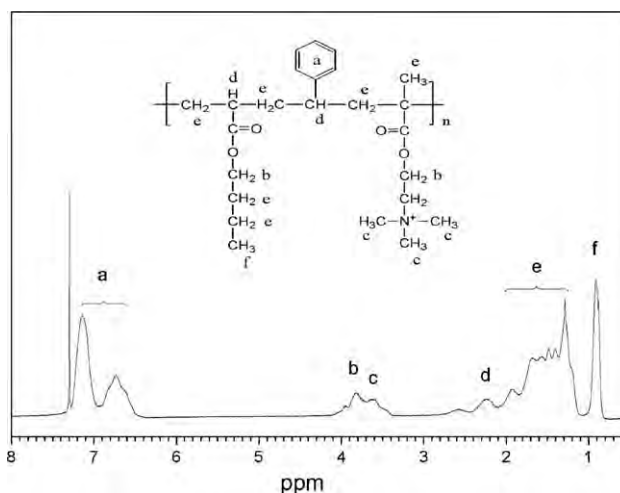


**Figure 2**  $^1\text{H-NMR}$  spectrum ( $\text{CDCl}_3$ ; 600 MHz) of P (St-BA-METAC) copolymer.

## RESULTS AND DISCUSSION

### Structure characterization of P (St-BA-METAC) copolymer

#### FTIR studies on P (St-BA-METAC) copolymer

The FTIR spectrum of the copolymer was shown in Figure 1. The peak at  $3440\text{ cm}^{-1}$  attributed to the stretching vibration of  $-\text{OH}$  in water absorbed by quaternary ammonium groups. The characteristic peaks at  $3028\text{ cm}^{-1}$  and  $1500\text{--}1600\text{ cm}^{-1}$  corresponded the stretching vibration of  $\text{C-H}$  and  $\text{C=C}$  bonds in the benzene ring, respectively. And those at  $760\text{ cm}^{-1}$  and  $699\text{ cm}^{-1}$  were the out-of-plane bending vibration of  $\text{C-H}$  in substituent benzene ring. The absorptions of  $\text{C=O}$  at  $1732\text{ cm}^{-1}$  and  $\text{C-O}$  at  $1164\text{ cm}^{-1}$  were observed correspondingly in the spectrum, confirming the presence of ester. The peak at  $1454\text{ cm}^{-1}$  corresponded the bending vibration of  $-\text{CH}_2$  in  $-\text{CH}_2-\text{N}^+(\text{CH}_3)_3$ . Otherwise, the strong absorption of  $-\text{CH}_3$  and  $-\text{CH}_2$  could be observed at  $2850\text{--}3000\text{ cm}^{-1}$ . The disappearance of characteristic  $\text{C=C}$  absorption of alkenes in the region of  $1620\text{--}1680\text{ cm}^{-1}$  indicated the well polymerization of all the monomers.

#### $^1\text{H-NMR}$ studies on P (St-BA-METAC) copolymer

The  $^1\text{H-NMR}$  spectrum of copolymer measured in  $\text{CDCl}_3$  was presented in Figure 2. As can be seen in the figure, the peaks at 6.5–7.2 ppm (a) attributed to the phenyl region of styrene. The broad peak at 3.82 ppm (b) was assigned to the  $-\text{CH}_2\text{O}-$ , whereas the one at 3.60 ppm (c) was assigned to  $-\text{N}^+(\text{CH}_3)_3$  of METAC. The peak at 0.91 ppm (f) was the protons of  $-\text{CH}_3$  in BA, and the peak at 2.28 ppm (d) was due to the  $-\text{CH}-$  in the backbones. The signals at 1.29–1.9 ppm (e) were other methyl and methylene

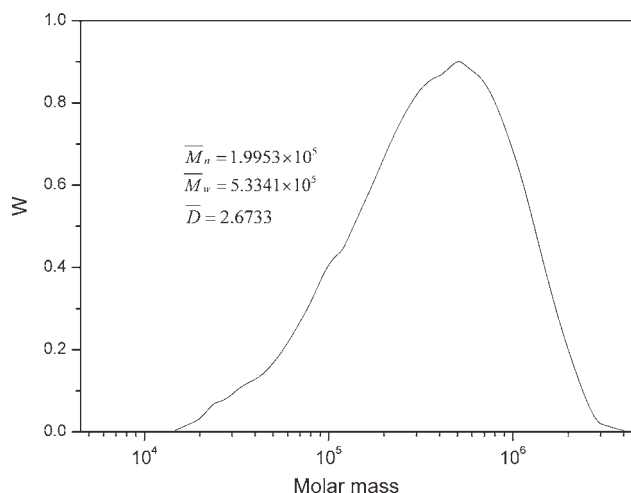


**Figure 3** Molecular weight and molecular weight distribution of P (St-BA-METAC) copolymer.

protons in the macromolecules. No signals for the protons associated with double bond of unreacted monomers can be detected in this  $^1\text{H-NMR}$  spectrum.

#### Molecular weight and molecular weight distribution of P (St-BA-METAC) copolymer

The molecular weight and molecular weight distribution of the copolymer were demonstrated by GPC, and the results were shown in Figure 3. The molecular weight of the copolymer determined by GPC was  $5.33 \times 10^5$  g/mol, and the molecular weight distribution ( $D = M_w/M_n$ ) was 2.67. The results of GPC indicated that the copolymerization of the monomers occurred, and the high molecular weight copolymer was obtained.

#### Interaction of cationic copolymer nanoparticles and BSA

##### Size and size distribution analysis

The size and size distribution of polymer nanoparticles were determined through PCS, and the effect of the concentration of BSA solution on the size and size distribution of polymer nanoparticles were investigated. Figure 4 showed the results of PCS measurement of the copolymer nanoparticles with different concentration of BSA solution. As can be seen from Figure 4, particle size of copolymer nanoparticles is 90 nm, with the PDI of 0.002. The particle size increased from 90 to 113 nm with the concentration of BSA solution varying from 0 to  $5.6 \times 10^{-7}$  mol/L, and the polydispersity index increased obviously as well.

The isoelectric point of BSA is around 4.6,<sup>22</sup> which is significantly lower than the pH value of measure environment. After mixing the polymer emulsion with the BSA solution, the BSA molecules presented

net negative charge. The adsorption of BSA and nanoparticles established through the electrostatic interaction between the cationic groups  $-\text{N}^+(\text{CH}_3)_3$  on the nanoparticles and the negative charged  $-\text{COO}^-$  in BSA molecule. Negative charged BSA molecules were adsorbed onto the surface of cationic nanoparticles, leading to the increase of the diameters of the nanoparticles. With the gradual increase of the BSA concentration, the adsorption to the particle surface came to saturation, leading the increase tendency of the particle size to slow. This can be seen from Figure 4. Because of the nonregularity of the adsorption, different amounts of BSA molecules were adsorbed onto each particle, causing a larger particle size distribution.

##### Zeta potential analysis

Figure 5 showed the zeta potential of free nanoparticles and nanoparticles loaded with BSA, measured at pH value of 7.4. The zeta potential of the blank polymer nanoparticles was +60.1 mV. The positive charge of the particles was attributed to the cationic groups  $-\text{N}^+(\text{CH}_3)_3$  on the particles. The zeta potential of pure BSA solution ( $1 \times 10^{-6}$  mol/L) was -16.8 mV, at the pH value much higher than its isoelectric point. Meanwhile, the zeta potential of nanoparticles decreased gradually from +58.4 to -4.68 mV as the BSA concentration increased from  $1 \times 10^{-8}$  to  $1 \times 10^{-6}$  mol/L. The addition of BSA resulted in a decrease in the zeta potential because of the load of negatively charged BSA causing the electrostatic bonding with  $-\text{N}^+(\text{CH}_3)_3$  on the particles.

##### TEM analysis

To get a better insight of the interactions between polymer nanoparticles with BSA, TEM were carried

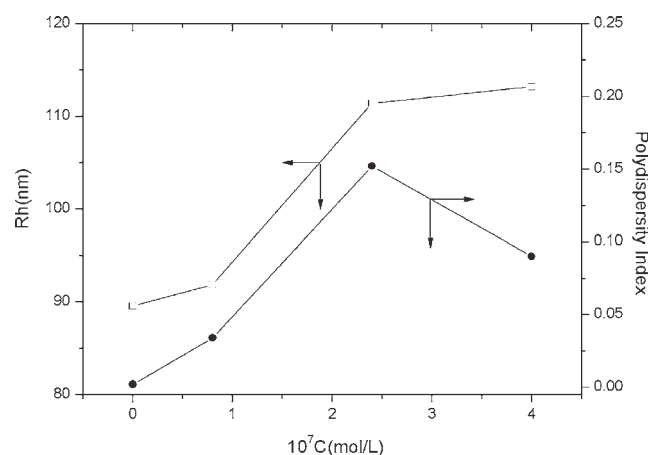


**Figure 4** Size (left) and size distribution (right) of copolymer nanoparticles with different concentration of BSA solution.

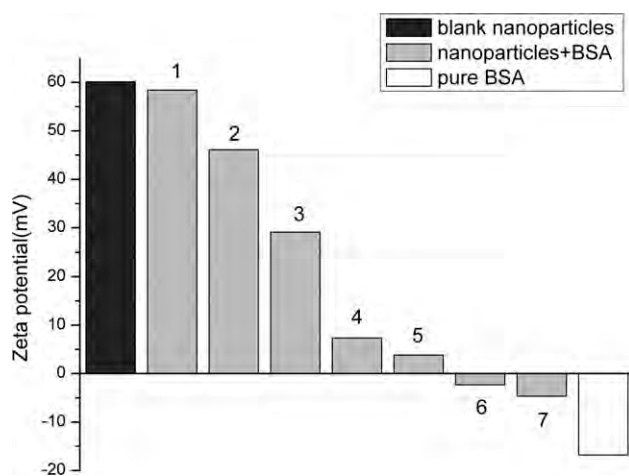
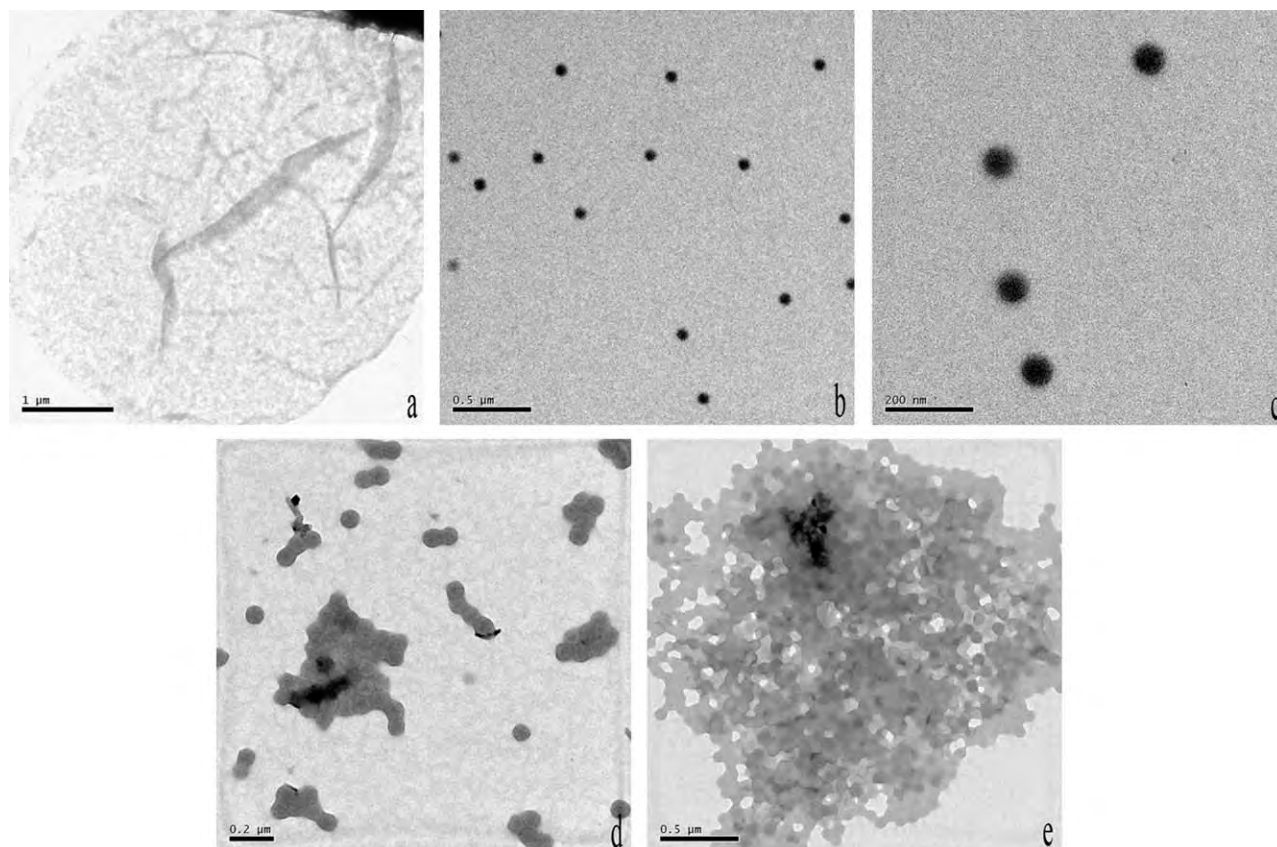


**Figure 5** Zeta potential of blank nanoparticles, pure BSA ( $1 \times 10^{-6}$  mol/L), and nanoparticles loaded with BSA (1–7:  $1 \times 10^{-8}$ ,  $1 \times 10^{-7}$ ,  $2 \times 10^{-7}$ ,  $4 \times 10^{-7}$ ,  $6 \times 10^{-7}$ ,  $8 \times 10^{-7}$ , and  $1 \times 10^{-6}$  mol/L) (pH = 7.4).

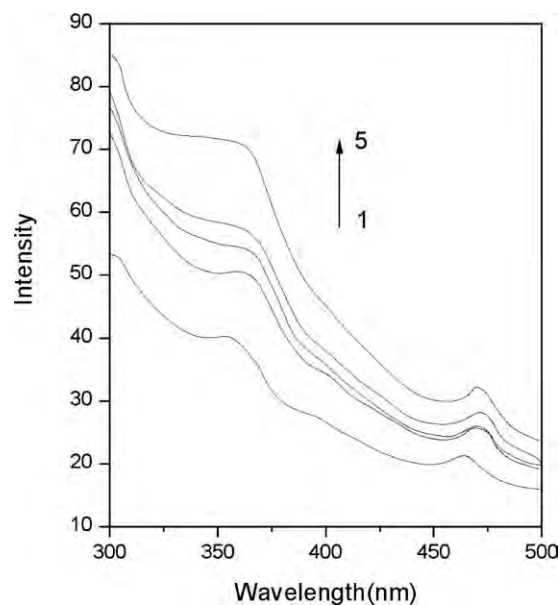
out to investigate the morphologies of polymer nanoparticles interacted with BSA. Figure 6(a) displayed the TEM image of pure BSA. BSA is a kind of crystalline protein<sup>23</sup>; the visual microstructures after evaporation of the solvent were observed from Figure 6(a).

Figure 6(b,c) showed the morphologies of copolymer nanoparticles obtained by emulsifier-free emulsion polymerization. Well-defined spherical nanoparticles with a narrow distribution and relatively clean surface can be clearly seen in the pictures, confirming that the nanoparticles were monodisperse along with the PCS results. The mean diameter of the nanoparticles was no larger than 90 nm, which was slightly smaller than the results measured by PCS attributed to the different measure fundamentals. It is the hydrodynamic diameter of the nanoparticles in the dispersed media that obtained by PCS, whereas TEM measures the diameters of the dry particles.<sup>24</sup>

The morphologies of nanoparticles interacted with BSA were shown in Figure 6(d,e) After the adsorption of BSA molecules onto the surface of nanoparticles, the colloid stabilization of nanoparticles was extremely affected. Therefore, nanoparticles exhibited high aggregation feature, which was quite different from pure nanoparticles themselves. As a result, nanoparticles might bind to each other and even conglomerate together during the process of evaporation of the solvent, as can be seen in Figure 6(d) and Figure 6(e), respectively.



**Figure 6** TEM images of (a) pure BSA, (b), (c) pure nanoparticles, and (d), (e) nanoparticles with BSA solution ( $0.8 \times 10^{-7}$ ,  $2.4 \times 10^{-7}$  mol/L).



**Figure 7** Fluorescence spectra of nanoparticles with different concentration of BSA solution:  $C_{BSA}$  (1–5): 0,  $0.8 \times 10^{-7}$ ,  $2.4 \times 10^{-7}$ ,  $4.0 \times 10^{-7}$ , and  $5.6 \times 10^{-7}$  mol/L (pH = 7.01).

### Fluorescence spectroscopy

Fluorescence spectroscopy was one of the most applied tools to investigate the interactions between proteins and foreign substances.<sup>25</sup> Determination of fluorescence properties enables analysis of microenvironmental changes during the process.<sup>26</sup> Figure 7 showed the fluorescent emission spectra of obtained emulsion in the presence of different concentration of BSA solution. Line 1 was the emission spectrum of pure emulsion without BSA solution. Because of the presence of benzyl and amino groups in the macromolecule, emission peaks at 353 nm and 463 nm can be observed from the emission spectrum. With the increasing of the concentration of BSA solution, the intensity of the peaks enhanced remarkably, with slight red shift of wavelength from 453 to 469 nm.

As mentioned above, BSA molecules were absorbed onto the surface of nanoparticles because of the electrostatic interaction of positive and negative charges. The interfaces of nanoparticles and water were obstructed by BSA molecules, so the nanoparticles were protected from the attack of polar water molecule, which may lead to the fluorescence quenching.<sup>27</sup> As the increase of the concentration of BSA solution, each nanoparticle was protected by more BSA molecules, leading to the intensity enhancement of emission spectrum.

### CONCLUSIONS

Cationic polymer nanoparticles were synthesized through emulsifier-free emulsion polymerization.

The quaternary ammonium groups were successfully introduced into the copolymer, which can be confirmed by the results of structure characterization through FTIR and  $^1\text{H-NMR}$  spectroscopy. The interaction of nanoparticles with BSA was investigated by PCS, TEM, and fluorescence spectroscopy. It was found that the obtained nanoparticles were well-defined spheres with clean surface, and the diameters of them were 90 nm. With the increase of concentration of BSA solution, the mean diameter of nanoparticles increased and the emission intensity of the nanoparticles enhanced significantly due to the electrostatic interaction of quaternary ammonium groups and negative charged BSA molecules.

### References

- Pichot, C. *Curr Opin Colloid Interface Sci* 2004, 9, 213.
- Choi, S. W.; Kim, W. S.; Kim, J. H. *J Disper Sci Technol* 2003, 24, 475.
- Ito, T.; Watanabe, J.; Takai, M.; Konno, T.; Iwasaki, Y.; Ishihara, K. *Colloids Surf B* 2006, 50, 55.
- Salvador-Morales, C.; Zhang, L.; Langer, R.; Farokhzad, O. C. *Biomaterials* 2009, 30, 2231.
- Xu, J. J.; Li, P.; Wu, C. *J Polym Sci Part A: Polym Chem* 1999, 37, 2069.
- Ramos, J.; Forcada, J. *J Polym Sci Part A: Polym Chem* 2005, 43, 3878.
- Boddohi, S.; Moore, N.; Johnson, P. A.; Kipper, M. J. *Biomacromolecules* 2009, 10, 1402.
- Kim, S. Y.; Shin, I. G.; Lee, Y. M. *Biomaterials* 1999, 20, 1033.
- Xu, X. J.; Chen, F. X. *J Appl Polym Sci* 2004, 92, 3080.
- Dziomkina, N. V.; Hempenius, M. A.; Vancso, G. J. *Eur Polym J* 2006, 42, 81.
- Alinec, B.; Arnoldova, P.; Frolik, R. *J Appl Polym Sci* 2000, 76, 1677.
- Sarrazin, P.; Beneventi, D.; Chaussy, D.; Vurth, L.; Stephan, O. *Colloids Surf A* 2009, 334, 80.
- Plank, J.; Gretz, M. *Colloids Surf A* 2008, 330, 227.
- Savage, N.; Diallo, M. S. *J Nanopart Res* 2005, 7, 331.
- Sumi, Y.; Shiroya, T.; Fujimoto, K.; Wada, T.; Handa, H.; Kawaguchi, H. *Colloids Surf B* 1994, 2, 419.
- Calvo, P.; Remuñán-López, C.; Vila-Jato, J. L.; Alonso, M. J. *J Appl Polym Sci* 1997, 63, 125.
- Slomkowski, S.; Basinska, T.; Miksa, B. *Polym Adv Technol* 2002, 13, 906.
- Srivastava, S.; Verma, A.; Frankamp, B. L.; Rotello, V. M. *Adv Mater* 2005, 17, 617.
- Ravindran, A.; Singh, A.; Raichur, A. M.; Chandrasekaran, N.; Mukherjee, A. *Colloids Surf B* 2010, 76, 32.
- Lynch, I.; Dawson, K. A. *Nanotoday* 2008, 3, 40.
- Simpson, R. J. *Proteins and Proteomics: A Laboratory Manual*; Cold Spring Harbor Laboratory Press: New York, 2003.
- Chaiyasut, C.; Tsuda, T. *Chromatography* 2001, 22, 91.
- Xiong, S. D.; Li, L.; Wu, S. L.; Xu, Z. S.; Chu, P. K. *J Polym Sci Part A: Polym Chem* 2009, 47, 4895.
- Liu, H.; Hu, X. X.; Wang, Y. X.; Li, X. Q.; Yi, C. F.; Xu, Z. S. *J Polym Sci Part A: Polym Chem* 2009, 47, 2892.
- Brown, M. P.; Royer, C. *Curr Opin Biotechnol* 1997, 8, 45.
- Ogawa, T.; Aoyagi, S.; Miyasaka, T.; Sakai, K. *Sensors* 2009, 9, 8271.
- Lu, M. L.; Wu, D. C.; Guo, N. *J Mater Sci: Mater Med* 2009, 20, 563.